# Hardware Implementation of Modified Backstepping Control for Sensorless Induction Motor Drive

Tarek Ameid[1,2], Hicham Talhaoui[3], Abdelkarim Ammar[4], Younes Azzoug[1,2], Remus Pusca[1], Raphaël Romary[1], Jean-Philippe Lecointe[1]
[1] *Univ.Artois, EA 4025 LSEE F-62400, Bethune, France*
[2] *Department of Electrical Engineering, Laboratory of Electrical Engineering of Biskra (LGEB), University of Biskra*
[3] *LPMRN Laboratory, Department of electromechanics*, *Bachir ElIbrahimi University, Bordj Bou Arreridj, Algeria*
[4] *Signals and Systems Laboratory*, *University of M'hamed Bougara, Boumerdes, Algeria*
tarek.ameid@ieee.org, hichem.talhaoui@univ-bba.dz, a.ammar@unive-boumerdes.dz, younes.azzoug@univ-biskra.dz, puscaremus@hotmail.com, raphael.romary@univ-artois.fr, jphilippe.lecointe@univ-artois.fr

***Abstract*—This paper presents a hardware implementation of sensorless Backstepping control for induction motor drive. The presented Backstepping control scheme has been designed in the stationary reference frame to reduce the control algorithm complexity. Furthermore, a full order Luenberger observer has been proposed for speed and torque estimation. Several operation conditions of the IM have been conducted such as load application, speed direction reversal and low-speed condition. In addition, an industrial benchmark test which comprises all speed condition has been done to check the control ability in different operation points. This work presents for the first time the experimental implementation of this developed control algorithm. The obtained experimental results prove the effectiveness and performance of the proposed control scheme.**

***Keywords—Induction motor, Backstepping control, Luenberger observer, dSpace 1104.***

## I. INTRODUCTION

The objectives of the various industrial structures are always linked to increasing quality, productivity and profitability. Three-phase squirrel-cage **I**nduction **M**otors (**IM**s) are widely used in variable speed drives, particularly in high-tech domains due to of their high power-to-weight ratio, robust structure, low purchase cost, and easy maintenance [1]. However, the difficulty of using IM in control-loop lies in the fact of the nonlinear coupled mathematical model, multivariable, which involves parameters that may vary with temperature, frequency, and other operating conditions. These constraints have significant effects on the accuracy of speed and torque control.

Many different methods are available for controlling IMs, which are distinguished by the motor performance they offer, but also by the cost of implementation. The Field-Oriented Control (FOC) has led to a radical change in control of the IMs. In this strategy, the torque and flux are decoupled by a suitable decoupling network and controlled independently by quadratic and direct stator currents respectively as a separately excited DC motor [2]. Unfortunately, the use of PI controllers needs particular information on control system modeling. Moreover, under these conditions, PI controllers have limitation provoked by the presence of time-varying parameters, disturbances, and uncertainties which affect the stability and the dynamic of the system [3]. Therefore, when the controlled part is subjected to strong non-linearities and time variables, the control algorithms must be designed to ensure the robustness of the process behavior with regard to uncertainties on the parameters and their variations.

The successful application of mathematical tools achieved a breakthrough development in the so-called robust and nonlinear control approaches to solving this problem and has made great progress recently. Non-linear controls offer several advantages like the good dynamic and the high-performance over linear control schemes. Various robust and nonlinear control strategies for IM drives have been proposed in the literature, like Sliding Mode Control (SMC) [4], the Input-Output Feedback Linearization control (IOFL) [5] and Backstepping Control (BC) [6]. The SMC adjustment is basically a method that forces the response to slide along a predefined trajectory. However, the chattering phenomena are the major disadvantage of this method [7]. Moreover, the IOFL provides an exact decoupling between system variables which preserves good behavior in dynamic states. However, the stability of this strategy cannot be guaranteed due to the presence of system uncertainties [8]. The BC is based on the tools of Lyapunov's stability, and offers a great flexibility in the syntheses. It has shown a fast dynamic response, easy implementation and robustness to parameters variation, and also for load torque disturbances [9]. The comparative study between integral and classical Backstepping in indirect field orientation based-control structures of the IM is presented in [10]. In [11] the rotor flux is recovered by using an adaptive sliding mode observer for the Backstepping driven IM. A field-programmable gate array (FPGA)-based implementation for an adaptive Backstepping control with radial basis function network (RBFN) observer is proposed in [12].

The control techniques cannot guarantee a good performance without the use of a suitable state observer. Many observer's structures have been associated with Backstepping control for different parameters estimation in order to minimize the cost of the control system by reducing the number of sensors. In [13], the Backstepping observer for the rotor speed estimation is presented. The authors in [14] propose a sensorless Backstepping control for the IM drive based on model reference adaptive system (MRAS) for rotor speed and rotor flux estimations.

Usually, the design of the Backstepping control is developed in the synchronous (d-q) reference frame in most works. It can be seen that the combination of Backstepping strategy with rotor field-orientation principle provides good control performance. However, the field-oriented reference frame requires the coordinate transformation which increases the complexity of the control's algorithm. Moreover, the

978-1-7281-4878-6/19/$31.00 ©2019 IEEE

estimation of flux position which is necessary for the transformation has some difficulties, particularly in the experimental implementation. Hence, to overcome this shortcoming, a proposed control scheme which developed in the stationary reference frame has been presented in [15], [16]. In [15], a combined control law between the traditional PI controllers and the Backstepping strategy has been presented, while an MRAS and sliding mode observers have been used for speed and flux component estimations for Backstepping-driven IM in [16]. However, in these works, only the simulation has been performed.

This paper is devoted to the nonlinear control of the induction machine. Mathematical modeling and experimental validation are investigated. The Backstepping control strategy is designed in the stationary reference frame in order to reduce the control algorithm complexity with keeping the same good propertied of the conventional Backstepping control. Moreover, a full order Luenberger observer has been used for rotor speed and torque estimations; investigate a sensorless control algorithm by decreasing the cost and improve the reliability of drive system. The proposed sensorless control is examined under different speed region operations. The obtained results show high robustness and good estimation accuracy in several modes of operation.

## II. MODEL OF THE IM

The dynamic equations of IM can be expressed as follows:

$$\dot{x} = Ax + Bu \tag{1}$$

with:

$$[x] = \begin{bmatrix} i_{s\alpha} & i_{s\beta} & \Phi_{r\alpha} & \Phi_{r\beta} \end{bmatrix}^T$$

$$[u] = [u_{s\alpha} \;\; u_{s\beta}]$$

$$A = \begin{bmatrix} -\lambda & 0 & \frac{\Gamma}{T_r} & \Gamma \cdot \omega \\ 0 & -\lambda & -\Gamma \cdot \omega & \frac{\Gamma}{T_r} \\ \frac{M}{T_r} & 0 & -\frac{1}{T_r} & -\omega \\ 0 & \frac{M}{T_r} & \omega & -\frac{1}{T_r} \end{bmatrix}; \quad \mathrm{B} = \begin{bmatrix} \delta & 0 \\ 0 & \delta \\ 0 & 0 \\ 0 & 0 \end{bmatrix}$$

where:

$$\begin{cases} \lambda = \frac{1}{T_s \cdot \sigma} + \frac{1}{T_r} \cdot \frac{1-\sigma}{\sigma} \\ \Gamma = \frac{1-\sigma}{\sigma} \cdot \frac{1}{M} \\ \delta = \frac{1}{\sigma \cdot L_s} \end{cases}, \quad \sigma = 1 - \frac{M^2}{L_s L_r}, \mathrm{T_s} = \frac{\mathrm{L_s}}{\mathrm{R_s}}, \mathrm{T_r} = \frac{\mathrm{L_r}}{\mathrm{R_r}}$$

The mechanical equations must also consider:

$$\begin{cases} C_e = P \cdot \frac{M}{L_s} (\Phi_{s\alpha} i_{s\beta} - \Phi_{s\beta} i_{s\alpha}) \\ J \cdot \frac{d\Omega}{dt} + \Omega \cdot f = C_e - C_r \end{cases} \tag{2}$$

with: $\Omega = \frac{\omega}{P}$

## III. BACKSTEPPING CONTROL OF IM

### A. First step

In the first step, the rotor speed and rotor flux module tracking error are defined by:

$$\begin{cases} e_1 = \Omega_{ref} - \Omega \\ \mathrm{z}_1 = \Phi_{ref}^2 - \Phi_r^2 \end{cases} \tag{3}$$

where $\Omega_{ref}$ and $\Phi_{ref}^2$ are present respectively the reference of speed and rotor flux modulus.

$$\Phi_r^2 = \Phi_{r\alpha}^2 + \Phi_{r\beta}^2 \tag{4}$$

Also, the error dynamic equations can be written by:

$$\begin{cases} \dot{e}_1 = \dot{\Omega}_{ref} - \left( \frac{\mu}{\mathrm{J}} (\Phi_{r\alpha} i_{s\beta} - \Phi_{r\beta} i_{s\alpha}) - \frac{f}{J} \Omega - \frac{C_r}{J} \right) \\ \dot{z}_1 = \frac{d}{dt} \left( \Phi_{ref}^2 \right) - 2 \frac{\mathrm{M}}{\mathrm{T_r}} (\Phi_{r\alpha} i_{s\alpha} + \Phi_{r\beta} i_{s\beta}) + 2 \frac{\Phi_r^2}{\mathrm{T_r}} \end{cases} \tag{5}$$

with: $\mu = P \cdot \frac{M}{L_s}$

By putting the virtual control expressions below,

$$\begin{cases} \alpha_1 = \Phi_{r\alpha} i_{s\beta} - \Phi_{r\beta} i_{s\alpha} \\ \beta_1 = \Phi_{r\alpha} i_{s\alpha} + \Phi_{r\beta} i_{s\beta} \end{cases} \tag{6}$$

We can write:

$$\begin{cases} \dot{e}_1 = \dot{\Omega}_{ref} - \left( \frac{\mu}{\mathrm{J}} \alpha_1 - \frac{f}{J} \Omega - \frac{C_r}{J} \right) \\ \dot{z}_1 = \frac{d}{dt} \left( \Phi_{ref}^2 \right) - 2 \frac{\mathrm{M}}{\mathrm{T_r}} \beta_1 + 2 \frac{\Phi_r^2}{\mathrm{T_r}} \end{cases} \tag{7}$$

Let us check the tracking error stability by choosing the Lyapunov Candidate Function (LCF) below:

$$\Gamma_1 = \frac{1}{2} e_1^2 + \frac{1}{2} e_2^2 \tag{8}$$

The derivative of this equation gives:

$$\dot{\Gamma}_1 = e_1 \dot{e}_1 + e_2 \dot{e}_2 \tag{9}$$

Let us consider the following virtual control reference that stabilizes the tracking errors $e_1$ and $z_1$:

$$\begin{cases} \alpha_{1\mathrm{ref}} = \frac{J}{\mu} \left( c_1 e_1 + \dot{\Omega}_{ref} + \frac{f}{J} \Omega + \frac{C_r}{J} \right) \\ \beta_{1ref} = \frac{T_r}{2M} \left( \mathrm{d}_1 \mathrm{z}_1 + \frac{d}{dt} \left( \Phi_{ref}^2 \right) + 2 \frac{\Phi_r^2}{\mathrm{T_r}} \right) \end{cases} \tag{10}$$

where $c_1 > 0$ and $d_1 > 0$ are the positive design gains that determine the dynamic of the closed loop.

so:

$$\begin{cases} \dot{e}_1 = -c_1 e_1 \\ \dot{z}_1 = -d_1 z_1 \end{cases} \tag{11}$$

$$\dot{\Gamma}_1 = -c_1 e_1^2 - d_1 z_1^2 \le 0 \tag{12}$$

This is evidently semi negative definite, so the tracking errors $e_1$ and $z_1$ have been stabilized.

*B.* Second step

Previous references, chosen to ensure a stable dynamic of speed- and flux-tracking error, cannot be imposed on the virtual controls without considering errors between them.

Let us define the following errors:

$$\begin{cases} e_2 = \alpha_{1ref} - \alpha_1 \\ z_2 = \beta_{1ref} - \beta_1 \end{cases} \tag{13}$$

One determines the new dynamics of the errors $e_1$ and $z_1$, expressed now in terms of $e_2$ and $z_2$, by:

$$\begin{cases} \dot{e}_1 = -c_1 e_1 + \dfrac{\mu}{J} e_2 \\ \dot{z}_1 = -d_1 z_1 + 2\dfrac{M}{T_r} z_2 \end{cases} \tag{14}$$

By deriving $e_2$ and $z_2$, we obtain the following error dynamics equations:

$$\begin{cases} \dot{e}_2 = \alpha_2 - \delta\left(\Phi_{r\alpha} u_{s\beta} - \Phi_{r\beta} u_{s\alpha}\right) \\ \dot{z}_2 = \beta_2 - \delta\left(\Phi_{r\alpha} u_{s\alpha} + \Phi_{r\beta} u_{s\beta}\right) \end{cases} \tag{15}$$

where:

$$\begin{cases} \alpha_2 = \dot{\alpha}_{1ref} + \left(\lambda + \dfrac{1}{T_r}\right)\alpha_1 + \omega\beta_1 + \kappa\omega\Phi_r^2 \\ \beta_2 = \dot{\beta}_{1ref} + \left(\lambda + \dfrac{1}{T_r}\right)\beta_1 - \omega\alpha_1 - \dfrac{\kappa}{T_r}\Phi_r^2 - \dfrac{M}{T_r}\left(i_{s\alpha}^2 + i_{s\beta}^2\right) \\ \omega = p\Omega \end{cases},$$

$$\kappa = \frac{M}{\sigma L_s L_r}$$

Now that the real control variables ( $u_{s\alpha}$ , $u_{s\beta}$ ) have appeared in this equation, we define the final complete LCF as follows:

$$\Gamma_2 = \frac{1}{2}e_1^2 + \frac{1}{2}z_1^2 + \frac{1}{2}e_2^2 + \frac{1}{2}z_2^2 \tag{16}$$

Thus, the LCF derivative is determined below,

$$\dot{\Gamma}_2 = -c_1 e_1^2 - d_1 z_1^2 - c_2 e_2^2 - d_2 z_2^2 + e_2\left(c_2 e_2 + \frac{\mu}{J} e_1 + \alpha_2 - \delta\left(\Phi_{r\alpha} u_{s\beta} - \Phi_{r\beta} u_{s\alpha}\right)\right) + z_2\left(d_2 z_2 + 2\frac{M}{T_r} z_1 + \beta_2 - \delta\left(\Phi_{r\alpha} u_{s\alpha} + \Phi_{r\beta} u_{s\beta}\right)\right) \tag{17}$$

where c2 and d2 are the positive design gains that determine the dynamics of the closed loop. In order to make the LCF derivative be negative definite and have the following expression:

$$\dot{\Gamma}_2 = -c_1 e_1^2 - d_1 z_1^2 - c_2 e_2^2 - d_2 z_2^2 \le 0 \tag{18}$$

We chose voltage control as follows:

$$\begin{cases} c_2 e_2 + \dfrac{\mu}{J} e_1 + \alpha_2 - \delta\left(\Phi_{r\alpha} u_{s\beta} - \Phi_{r\beta} u_{s\alpha}\right) = 0 \\ d_2 z_2 + 2\dfrac{M}{T_r} z_1 + \beta_2 - \delta\left(\Phi_{r\alpha} u_{s\alpha} + \Phi_{r\beta} u_{s\beta}\right) = 0 \end{cases} \tag{19}$$

And then we obtain the input controls, ( $u_{s\alpha}$ , $u_{s\beta}$ ):

$$\begin{cases} u_{s\alpha} = \dfrac{1}{\delta\Phi_r^2}\left[B_b\Phi_{r\alpha} - A_b\Phi_{r\beta}\right] \\ u_{s\alpha} = \dfrac{1}{\delta\Phi_r^2}\left[B_b\Phi_{r\beta} + A_b\Phi_{r\alpha}\right] \end{cases} \tag{20}$$

where:

$$\begin{cases} A_b = c_2 e_2 + \dfrac{\mu}{J} e_1 + \alpha_2 \\ B_b = d_2 z_2 + 2\dfrac{M}{T_r} z_1 + \beta_2 \end{cases}$$

## IV. SENSORLESS CONTROL ALGORITHM

The Luenberger state observer for estimating the stator current and the rotor flux, using the measured stator currents and voltages, is described by the following set of equations:

$$\begin{cases} \dot{\hat{x}} = (A - LC)\hat{x}(t) + Bu + L\hat{y} \\ \hat{y}(t) = C\hat{x}(t) \end{cases} \tag{21}$$

with: $[\hat{x}] = \left[\hat{i}_{\alpha s} \quad \hat{i}_{\beta s} \quad \hat{\Phi}_{\alpha r} \quad \hat{\Phi}_{\beta r}\right]^T$ , $[y] = \left[i_{s\alpha} \quad i_{s\beta}\right]^T$ ,

$[\hat{y}] = \left[\hat{i}_{s\alpha} \quad \hat{i}_{s\beta}\right]^T$ , $C = \begin{bmatrix} 1 & 0 & 0 & 0 \\ 0 & 1 & 0 & 0 \end{bmatrix}$

where ^ denotes the estimated values, $\hat{x}(t)$ is the observer state vector and L is the observer gain matrix, which is selected so that the system will be stable [17]. The principle of the observer diagrams is presented in Fig. 1.

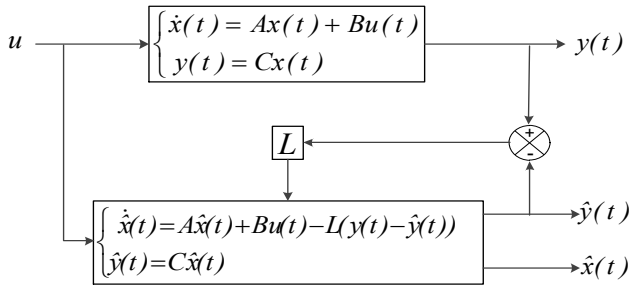


Fig. 1. Principle of the observer diagrams

To ensure that the estimation error vanish over time for any, $\hat{x}(0)$ we should select the observer gain matrix L so that (A-LC) is asymptotically stable. Therefore, the observer gain matrix should be chosen so that all Eigen values of (A-LC) have negative real parts.

The gain matrix L is defined as follows:

$$L=\begin{bmatrix} g_{L1} & g_{L2} & g_{L3} & g_{L4} \\ -g_{L2} & g_{L1} & -g_{L4} & g_{L3} \end{bmatrix}^T$$

where:

$$g_{L1}=(k_g-1)\left(\frac{R_s}{\sigma L_s}+\frac{1-\sigma}{\sigma T_r}+\frac{1}{T_r}\right);\quad g_{L2}=(k_g-1)\hat{\omega};$$

$$g_{L3}=\left(\frac{1-k_g^2}{a_L}\right)\left(\frac{1}{\sigma T_s}+\frac{1-\sigma}{\sigma T_r}+\frac{a_L}{T_r}\right)+\left(\frac{k_g-1}{a_L}\right)\left(\frac{1}{\sigma T_s}+\frac{1-\sigma}{\sigma T_r}+\frac{1}{T_r}\right);$$

$$g_{L4}=\frac{(k_g-1)}{a_L}\hat{\omega}.$$

with: $a_L=\dfrac{M}{\sigma L_{sc}L_{rc}}$ and $(k_g\geq 1)$

According to Lyapunov's theory, the adaptive scheme for speed estimation is given by:

$$\hat{\omega}=k_p(e_{is\alpha}.\Phi_{r\beta}-e_{isb}.\Phi_{r\alpha})+k_i\int(e_{is\alpha}.\Phi_{r\beta}-e_{isb}.\Phi_{r\alpha})dt \quad (22)$$

where:

$e=x-\hat{x}$,

$k_p$ and $k_i$ are respectively the proportional and integral constants.

## V. Experimental Implementation

The experimental test bench of control is shown in Fig. 2. The control algorithm is implemented using dSpace DS1104 R&D controller board with control desk and Matlab/Simulink software package. The test bench is composed of: an IM of 1.1 kW, dSpace DS 1104 with control desk software plugged into the computer, a power electronics SEMIKRON converter with a rectifier and an IGBT inverter, a magnetic powder brake with load control unit, a speed sensor (incremental encoder), Hall's type current and voltage sensors and an autotransformer (0-450V). The specifications for the IM with corresponding parameters are given in appendix.

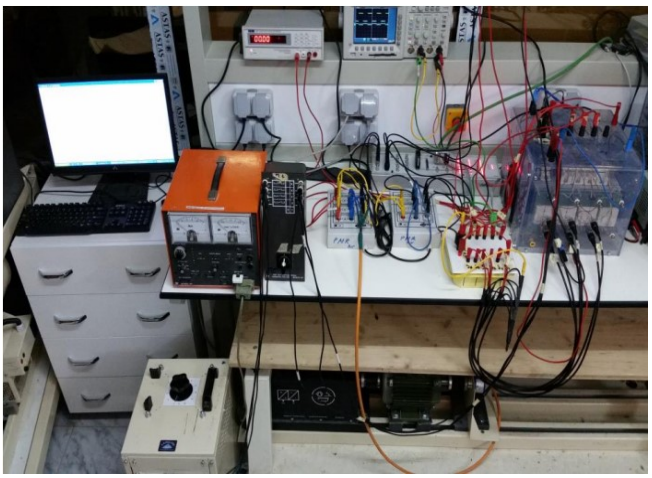

Fig. 2. Test bench of the Backstepping control.

## VI. Application and Results

The figures below show the experimental results of the sensorless Backstepping control of the IM drive based on the Luenberger observer. The chosen sampling frequency for the Real-Time implementation is *10kHz*.

### A. *Reference tracking test:*

a benchmark reference trajectory is chosen in order to test the robustness of the IM control vis-a-vis to speed tracking undervalues (0, 100, 300, 1200, -954.92, 0, 50 rpm), as presented in Fig. 3.

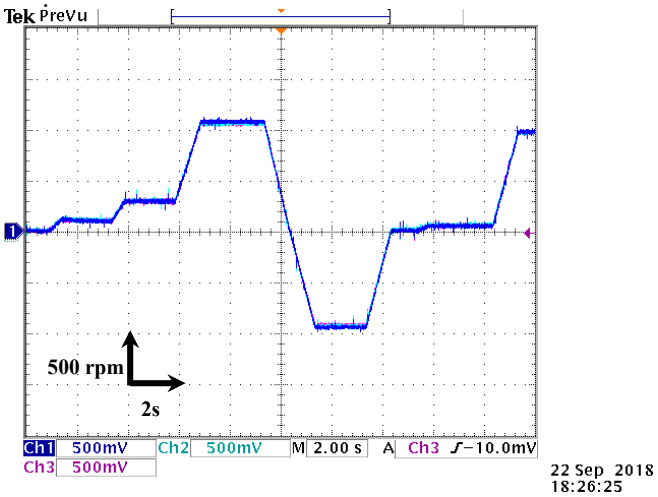


Fig. 3. Speed response according to the reference trajectory

The experimental result shows the good performance of the backstepping control without speed sensor using the Luenberger observer for trajectory monitoring and disturbance rejection. The estimated and actual speeds converge towards the reference speed at the same time. The Luenberger observer gives a good estimate of the speed in the different operating regions.

The test of speed direction reversing has been employed in the figure below (Fig. 4). The speed reference is changing from (±1000 rpm). The Fig. 4a illustrates from the top to the bottom the rotor speed (1div=1000rpm) and the electromagnetic torque (1div=10N.m). Next in Fig. 4b, the stator flux components, flux magnitude and angle position are depicted respectively.

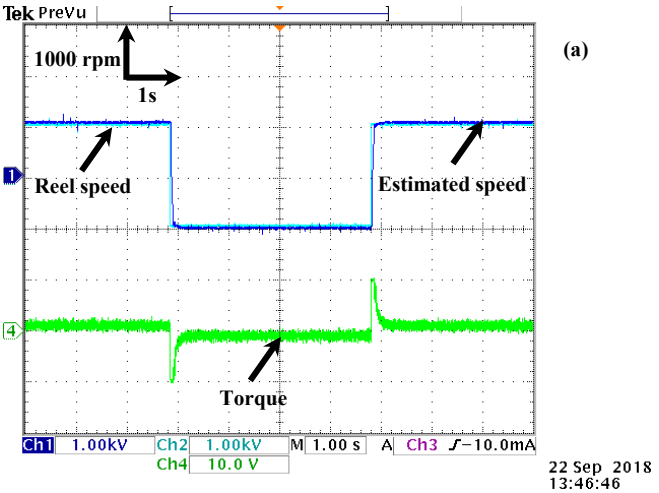

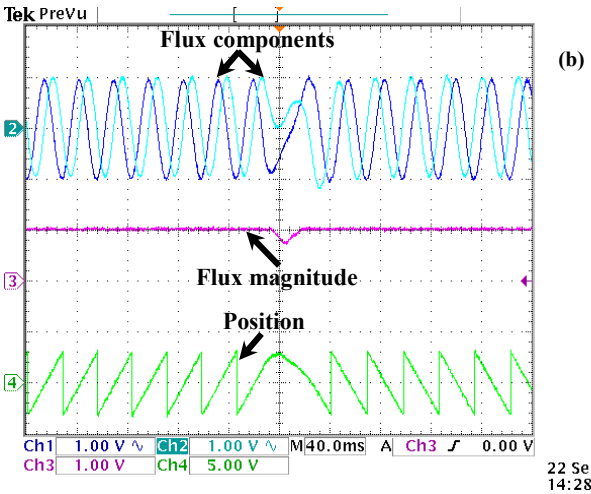


Fig. 4. Speed reversal tests, (a) speed and torque (b) flux components, flux magnitude and angel position.

As it can be seen from Fig. 4a, the Backstepping control presents good speed response at different operation points and provides a considerable reduction in torque ripples.

Further, in Fig. 4b the stator flux components illustrate a good sinusoid and smooth waveform. Then, the flux magnitude has shown low ripples and fast tracking to its reference's value of *1Wb*. Finally, the angel position is presented in the bottom to indicate the rotation sense and frequency.

### *B. Starting up, steady state and load application*

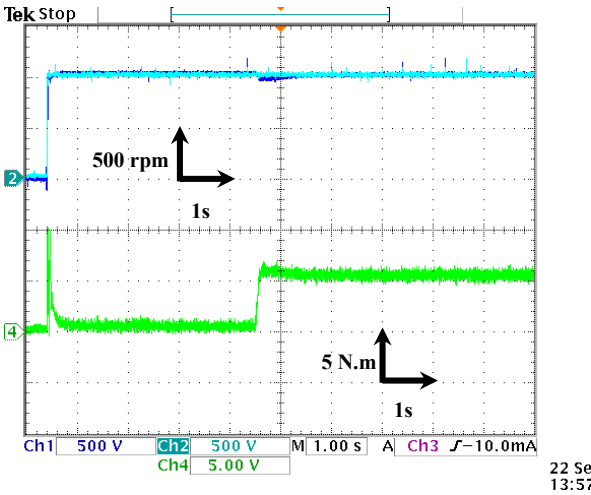


Fig. 5. Rotor speed and torque with rated load application

The rotor speed and torque evolution are presented in Fig. 5. The results clearly show that the speed converges rapidly towards its reference without overshooting. The perturbation caused by the application of the load is quickly eliminated. The electromagnetic torque is reacting very quickly to load variations without reaching an unacceptable value.

Fig. 6 presents the stator phase currents, it can be seen that the stator phase currents have a good dynamic and balanced sinusoid waveform.

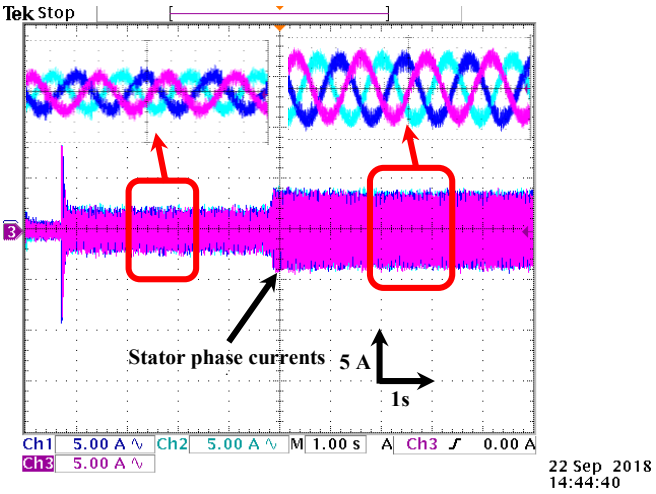


Fig. 6. Stator phase currents with rated load application

## VII. CONCLUSION

In this paper, the experimental validation of a sensorless nonlinear Backstepping control for IM drive is performed. The stationary reference frame-based model has been used for the control algorithm design. Furthermore, the full order Luenberger observer has been applied for rotor speed and torque estimation a sensorless control algorithm. The effectiveness of the global control strategy was examined through the experimental implementation. The obtained results show the high performance and the good dynamics of the proposed control algorithm during different operation condition. Moreover, the Luenberger observer offers an accurate speed estimation which improves the reliability of sensorless control. The use of stationary reference frame-based model reduces the control algorithm complexity and overcome the problem position estimation while keeping the same good properties of the backstepping control.

As a perspective of this paper, the Backstepping control based on stationary reference frame model will be designed for the fault tolerance control of the IM, diagnosis in closed-loop drive and efficiency optimization algorithm based on losses minimization.

## APPENDIX

| | |
|---|---|
| Type | 3-phase squirrel-cage |
| Rated Power | 1,1 kW |
| Number of pole pairs | 2 |
| Rated Speed | 1450 rpm |
| Rated Stator Current | 2,5 A |
| Rated RMS phase voltage | 400 V |
| Stator resistance | 6.75 Ω |
| Rotor resistance | 6.21 Ω |
| Stator inductance | 0.5192 H |
| Rotor inductance | 0.5192 H |
| Mutual inductance | 0.4757 H |
| Inertia moment | 0.0124 kg.m$^2$ |
| damping coefficient | 0.0029*N.m/rad/s* |

## REFERENCES


[1] S. K. Sahoo and T. Bhattacharya, "Field weakening strategy for a vector-controlled induction motor drive near the six-step mode of operation," IEEE Trans. Power Electron., vol. 31, no. 4, pp. 3043–3051, 2016.

[2] D. Casadei, F. Profumo, and A. Tani, "FOC and DTC: two viable schemes for induction motors torque control," IEEE Trans. Power Electron., vol. 17, no. 5, pp. 779–787, Sep. 2002.

[3] A. Ammar, "Performance improvement of direct torque control for induction motor drive via fuzzy logic-feedback linearization," COMPEL - Int. J. Comput. Math. Electr. Electron. Eng., p. COMPEL-

04-2018-0183, Apr. 2019.

[4] A. Benchaib, A. Rachid, and E. Audrezet, “Sliding mode input-output linearization and field orientation for real-time control of induction motors,” IEEE Trans. Power Electron., vol. 14, no. 1, pp. 3–13, 1999.

[5] F. Alonge, M. Cirrincione, M. Pucci, and A. Sferlazza, “Input-output feedback linearization control with on-line MRAS-based inductor resistance estimation of linear induction motors including the dynamic end effects,” IEEE Trans. Ind. Appl., vol. 52, no. 1, pp. 254–266, 2016.

[6] H. Echeikh, R. Trabelsi, M. F. Mimouni, A. Iqbal, and R. Alammari, “High performance backstepping control of a fivephase induction motor drive,” in 2014 IEEE 23rd International Symposium on Industrial Electronics (ISIE), 2014, pp. 812–817.

[7] A. Guezmil, H. Berriri, R. Pusca, A. Sakly, R. Romary, and M. F. Mimouni, “Experimental Investigation of Passive Fault Tolerant Control for Induction Machine Using Sliding Mode Approach,” Asian J. Control, vol. 21, no. 1, pp. 520–532, Jan. 2019.

[8] C. Lascu, S. Jafarzadeh, M. S. Fadali, and F. Blaabjerg, “Direct Torque Control With Feedback Linearization for Induction Motor Drives,” IEEE Trans. Power Electron., vol. 32, no. 3, pp. 2072–2080, Mar. 2017.

[9] M. Moutchou, A. Abbou, and H. Mahmoudi, “Sensorless speed backstepping control of induction machine, based on speed MRAS observer,” Proc. 2012 Int. Conf. Multimed. Comput. Syst. ICMCS 2012, no. Im, pp. 1019–1024, 2012.

[10] M. Fateh and R. Abdellatif, “Comparative study of integral and classical backstepping controllers in IFOC of induction motor fed by voltage source inverter,” Int. J. Hydrogen Energy, vol. 42, no. 28, pp. 17953–17964, Jul. 2017.

[11] R. Trabelsi, A. Khedher, M. F. Mimouni, and F. M’Sahli, “Backstepping control for an induction motor using an adaptive sliding rotor-flux observer,” Electr. Power Syst. Res., vol. 93, pp. 1–15, 2012.

[12] L.-T. Teng, Y.-C. Hung, F.-J. Lin, and C.-Y. Chen, “FPGA-based adaptive backstepping control system using RBFN for linear induction motor drive,” IET Electr. Power Appl., vol. 2, no. 6, pp. 325–340, Nov. 2008.

[13] A. Zaafouri, C. Ben Regaya, H. Ben Azza, and A. Châari, “DSP-based adaptive backstepping using the tracking errors for high-performance sensorless speed control of induction motor drive,” ISA Trans., vol. 60, pp. 333–347, 2016.

[14] T. Ameid, A. Menacer, H. Talhaoui, A. Ammar, and Y. Azzoug, “Sensorless speed estimation and backstepping control of induction motor drive using model reference adaptive system,” in 2017 5th International Conference on Electrical Engineering - Boumerdes (ICEE-B), 2017, pp. 1–6.

[15] O. Benzineb, H. Salhi, M. Tadjine, M. S. Boucherit, and M. Benbouzid, “A PI / Backstepping Approach for Induction Motor Drives Robust Control,” in International Review of Electrical Engineering, 2010, 5 (2), pp.426-432. ⟨hal-00526614⟩, 2010.

[16] M. MOUTCHOU, A. ABBOU, and H. MAHMOUDI, “MRAS-based sensorless speed backstepping control for induction machine, using a flux sliding mode observer,” TURKISH J. Electr. Eng. Comput. Sci., vol. 23, pp. 187–200, 2015.

[17] H. Chalawane, A. Essadki, and T. Nasser, “MRAS and Luenberger observers using a SIFLC controller in adaptive mechanism based sensorless fuzzy logic control of induction motor,” in 2016 International Conference on Electrical and Information Technologies (ICEIT), 2016, no. 1, pp. 153–158.